TRANSPORT STUDIES DURING SAWTEETH AND H-MODES ON JET USING LASER ABLATION.

N Hawkes[a], Z Wang, R Barnsley, K Behringer[b], S Cohen[c], B Denne, A Edwards, R Giannella, R Gill, G Magyar, D Pasini, N Peacock[a], U Schumacher[b], C Vieider[d] and D Zasche[b]

JET Joint Undertaking, Abingdon, Oxon, OX14 3EA, UK
[a] *UKAEA Culham Lab., Abingdon, Oxon, OX14 3DB,* UK
[b] *Max-Planck-Institut fur Plasmaphysik, D-8046, Garching,* FRG
[c] *Plasma Physics Laboratory, Princeton Univ., Princeton, NJ 08544,* USA
[d] *Uppsala Institute of Technology,* SWEDEN

A system for the controlled injection of trace impurities by laser ablation has recently been commissioned on JET. Small amounts of metallic impurities have been injected in order to study transport phenomena. In all cases the amounts, corresponding to an injected quantity of a few 10^{18} atoms (an impurity concentration of 0.01% of n_e), were sufficiently small to avoid perturbing any plasma parameter apart from the radiation ($\Delta P_{rad} < 0.5$ MW). We report here on measurements of impurity confinement time (τ_{imp}) and observations of impurity transport effects using this technique.

A suite of spectrometers viewing fixed lines of sight was used to gather information on the time behaviour of a range of ionisation stages. In addition measurements of the soft X-ray emission were obtained with good spatial and temporal resolution from two X-ray cameras.

Sawteeth observations - The soft X-ray cameras show inverted sawteeth during the rise phase of radiation from injected impurities. Figure 1 shows the time development of the central chord soft X-ray signal and central electron temperature (T_e) illustrating the inversion of the first sawtooth after impurity injection.

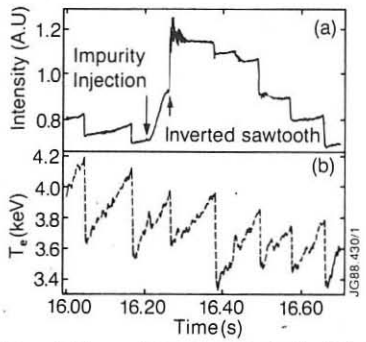

Figure 1. Time evolution of central chord soft X-ray signal (a) and electron temperature (b) during a discharge with Mo injection.

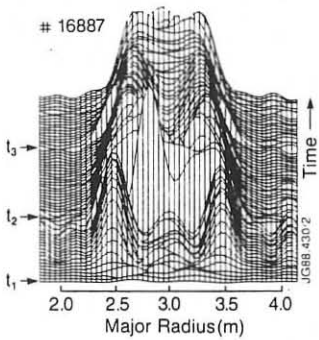

Figure 2. Time evolution of the injected impurity X-ray emission distribution along the horizontal central chord: t_1, impurity injection, t_2, t_3 sawtooth crashes (Shot 16887).

Clearly the increase in radiation due to the influx of impurities into the central region of the plasma at the time of the sawtooth crash overcompensates the drop in T_e. In most cases the inverted sawtooth is accompanied by a large amplitude $m = 1$ oscillation. This oscillation usually disappears within less than half a sawtooth period. During this time the amplitude of the oscillation decays gradually. Their frequency also decreases, from 500 Hz immediately after the sawtooth crash to 400 Hz as the oscillation disappears. A clear understanding of these oscillations is still lacking.

Tomographic reconstruction of the plasma emissivity reveals that impurity transport within the central region (inside the $q = 1$ surface) is profoundly different from that in the rest of the plasma. Figure 2 shows a sequence of radial emission profiles from the same discharge for times after the ablation. Background radiation, present before ablation, has been subtracted out. Immediately after ablation the radiation profile builds up at mid radius, with no growth in radiation from the centre. This central region, inside $q = 1$, only fills in when a sawtooth crash occurs, time t_2 in the figure. The filling is incomplete even after the first crash, it taking typically two to three sawtooth cycles for the intially hollow profile to become peaked on axis. The radiation profiles indicate that rather than a transport barrier at $q = 1$, impurity transport inside the $q = 1$ region is reduced, there being only a slow evolution of the radiation profile in this zone between sawtooth crashes. During the decay phase the reverse situation applies in that impurities linger in the central region, again only crossing $q = 1$ at the time of the sawtooth crash.

Scaling studies - Scaling studies were performed in ohmic L-mode shots of the decay time of XUV radiation intensity from high ionization stages (ionisation energies typically > 1 KeV) of the injected metals. Such radiation is emitted from the outer 1/3rd of the plasma radius. At this radius the decay time of the intensity is representative of the global impurity containment time (τ_{imp}). The decay curves of the intensity were corrected for variations in T_e and n_e with the application of an empirical correction formula derived from modelling calculations performed with an impurity transport code. The corrected decay curves were then fitted by an exponential to give the decay time and the resulting times stored in a database. The X-ray observations indicate that diffusion of impurities inside $q = 1$ is much lower than in the outer regions but since transport is effectivly enhanced during the sawtooth crash and the decay times span many sawtooth cycles the times we measure are governed by the transport in the region outside $q = 1$.

No dependence of τ_{imp} with charge of the ablated ions was detected, thus simplifying the further analysis of the data. An apparent scaling of τ_{imp} with density was observed in the data (figure 3) with the form $.09(n_e/10^{19})^{.4}\sqrt{q_L}$. However with the parameter range explored it is not yet possible to rule out other dependencies. τ_{imp} and the energy confinement time, τ_E, were found to be uncorrelated. In particular no reduction in τ_{imp} with auxilliary heating was detected (up to $P_{tot} < 15$ MW) although the number of heated shots studied was limited. During H-mode, however, the impurity confinement time became much longer than under any other operating condition, exceeding τ_E.

Transport in H-mode - Our dataset includes two observations of impurity transport during H-mode which we have modelled using an impurity transport code. In a 4MA

shot, 18627, cobalt was injected into the discharge at 12s, 0.5s after the start of the H-mode. Figure 4 shows the time traces of the injected Co as well as the time traces of the intrinsic impurities nickel and oxygen.

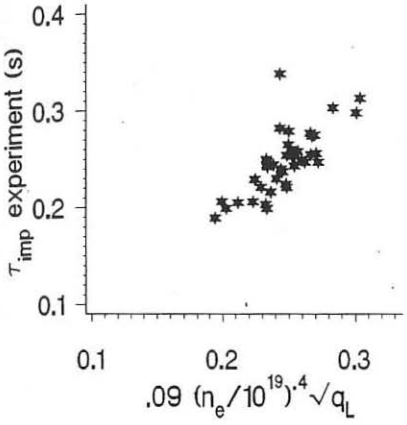

Figure 3. Scaling of t_{imp} with volume average electron density and safety factor.

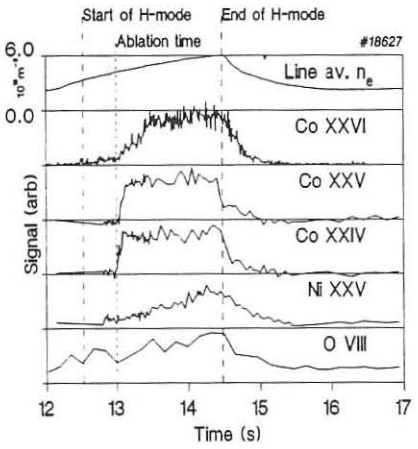

Figure 4. Time development of injected Co and intrinsic Ni and O during an H-mode (Shot 18627).

The emission from the lower ionisation stages of Co rises rapidly (within 0.1s) to a steady value which persists up to the end of the H-mode. The lower stages of C and O show little effect of the H-mode whereas OVIII and CVI (ionisation energies 870 and 490 eV) behave like the nickel lines /1/ (ionisation energies > 2000 eV) and ramp up during the H-mode. The bulk plasma therefore behaves as an almost ideal 'integrator' of impurities. Adjustment of the raw signal intensities to take account of the changing n_e and T_e modifies the near rectangular Co XXIV and Co XXV time traces, giving them a slow decay with time, leading to the plasma being described better as a slightly 'leaky' integrator with confinement time of 4s ($> > \tau_E$).

A transport model describing the behaviour of intrinsic impurities during H-mode had previously been proposed /2/. This model accounted for the time development of radiation from iron injected near the H-mode transition of a 3MA shot (17068) (giving an impurity decay time of 0.8s - nearly equal to τ_E). To account for the data in figure 4, however, it is necessary to include a stronger inwards convection (V) at the very edge of the plasma. The profiles of diffusion (D) and V adopted for the modelling are shown in figure 5 and the resulting time evolution of Co, Ni and O radiation in figure 6 which well describe the experimental observations. The lower ionisation stages of oxygen lie in the scrape off (or in the region of inwards convection) and hence do not see the impurity build up of the bulk plasma.

The neoclassical transport description of Hirshman and Sigmar /3/ as evaluated by Fussmann /4/ is implemented in the transport code allowing comparisons to be made with our coefficients. The crucial feature in our model is the ratio of V/D (~ 50 m^{-1}) at the plasma edge. Whilst the $\nabla n_i/n_i$ terms of the drift (arising out of the steep edge

density gradients) are of approximately the correct shape the $\nabla T_i/T_i$ screening terms are hard to estimate from the T_i profiles. The neoclassical ratio V/D is plausibly comparable with our model ratio. The D profile is not a sensitive parameter in the model and the profile selected is greater than the neoclassical diffusion by a factor varying between 3 in the centre and 50 at the edge. The choice of a lower D value leads to a slower penetration by impurities of the core plasma and thus gives a slower rate of rise of emission from (particularly) Co XXVI. The effect of sawteeth has not been included, however, in this model and will act to mitigate this slower rise.

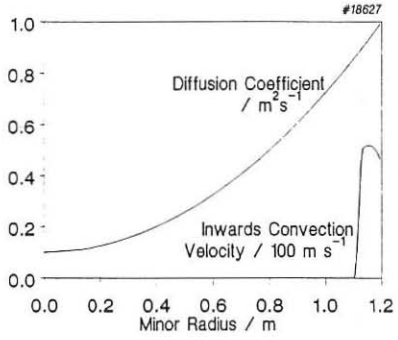

Figure 5. Transport parameters used in modelling.

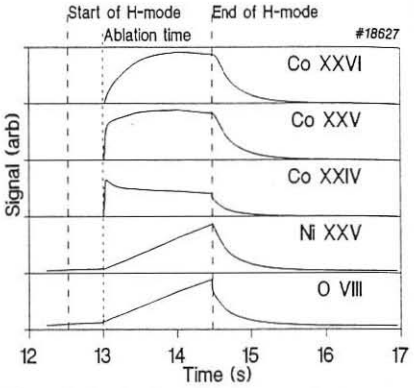

Figure 6. Results of modelling. A correction for density variation has been applied.

Conclusions - Laser ablation of test impurities into JET plasmas has demonstrated a significant reduction of transport within the $q = 1$ surface as well as the expected increase in transport during a sawtooth crash. Studies of the variation of τ_{imp} with plasma parameters have yielded a scaling model but it cannot yet be regarded as complete.

Studies of H-mode plasmas extend observations of intrinsic impurity behaviour and confirm the significance of the edge (within 0.2m of the separatrix) with respect to the retention of impurities. Whilst not adequately described by neoclassical transport there are enough similarities to encourage further investigation in this direction. The particular effects of the neutral beam driven momentum source and the non circularity of the minor cross-section are not included in the neoclassical description adopted here.

References

/1/ Giannella R. *et al.* this conference.
/2/ Behringer K *et al.* EPS Dubrovnik in Europhys. Conf. Abs. **12B** I p338.
/3/ Hirshman S.P. and Sigmar D.J. Nucl. Fus **21** (1981) 1079
/4/ Fussmann G. *et al.* J. Nucl. Mater. in print (1988) (8th PSI, Jülich 1988)